



Fluxes of CO₂, CH₄, and N₂O in tundra-covered and Nothofagus forest soils in the Argentinian Patagonia

Mariana Médice Firme Sá ^a, Carlos Ernesto G.R. Schaefer ^b, Diego C. Loureiro ^c, Felipe N.B. Simas ^d, Bruno J.R. Alves ^a, Eduardo de Sá Mendonça ^e, Eduardo Barretto de Figueiredo ^f, Newton La Scala Jr ^g, Alan R. Panosso ^{g,*}

^a Brazilian Agricultural Research Corporation, Embrapa Agrobiology, Rodovia BR 465, km 7, 23891-000 Seropédica, RJ, Brazil

^b Department of Soils, Federal University of Viçosa—UFV, Avenida Peter Henry Rolfs s/n, 36570-000 Viçosa, MG, Brazil

^c Department of Agricultural Engineering, Federal University of Sergipe—UFS, Avenida Marechal Rondon s/n, 49100-000 São Cristóvão, SE, Brazil

^d Department of Education, Federal University of Viçosa—UFV, Avenida Peter Henry Rolfs s/n, 36570-000 Viçosa, MG, Brazil

^e Department of Plant Production, Federal University of Espírito Santo—UFES, Alto Universitário, s/n, 29500-000 Alegre, ES, Brazil

^f Department of Rural Development - DDR, Federal University of São Carlos—UFSCAR, Rodovia Anhanguera, km 174 - SP-330, 13600-970 Araras, SP, Brazil

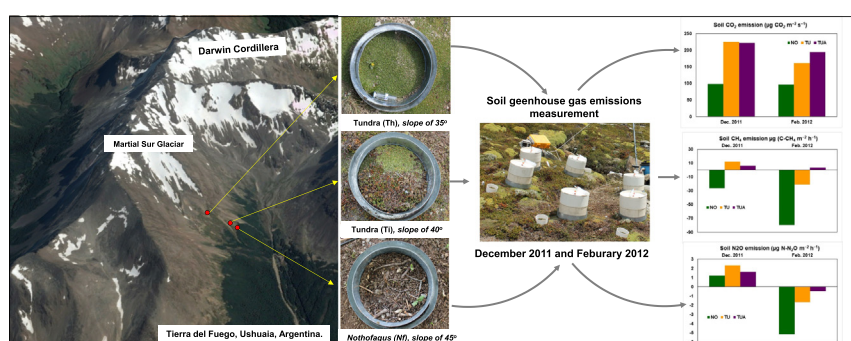
^g Department of Exact Sciences, São Paulo State University—FCAV/UNESP, Via de Acesso Prof. Paulo Donato Castellane s/n, 14884-900 Jaboticabal, SP, Brazil



HIGHLIGHTS

- Soil CO₂ emission presented a high positive correlation with soil temperature.
- Tundra covered soil presented the highest greenhouse gases fluxes in relation to the forest.
- Forest soils represent large drains of N₂O from the atmosphere.
- Tundra covered soils present a greater environmental fragility.

GRAPHICAL ABSTRACT



ARTICLE INFO

Article history:

Received 12 September 2018

Received in revised form 17 December 2018

Accepted 21 December 2018

Available online 22 December 2018

Editor: Ralf Ludwig

Keywords:

GHG emissions

Tierra del Fuego

Climate change

ABSTRACT

While most soils in periglacial environments present high fluxes of CO₂ (F_{CO2}), CH₄ (F_{CH4}), and N₂O (F_{N2O}), few of them have a tendency to drain greenhouse gases from the atmosphere. This study aimed to assess greenhouse gas fluxes at different sub-Antarctic sites and time periods (at the beginning of thaw and height of summer). To investigate the time of year effect on greenhouse gas emissions, F_{CO2}, F_{CH4}, and F_{N2O} were measured at two sites tundra-covered (Ti and Th) and Nothofagus forest soil (Nf) on Monte Martial, at the southernmost tip of South America, Tierra del Fuego, Argentina. F_{CO2} ranged from 96.33 to 225.72 $\mu\text{g CO}_2 \text{ m}^{-2} \text{ s}^{-1}$ across all sites and periods, showing a positive correlation with soil temperature (Ts) (4.1 and 8.2 °C, respectively) ($r^2 > 0.7$; $p < 0.05$). The highest values of F_{CO2} were found at Ti and Th (728.2 and 662.64 $\mu\text{g CO}_2 \text{ m}^{-2} \text{ s}^{-1}$, respectively), which were related to higher temperatures (8.2 and 8.6 °C, respectively) when compared to those of Nf. For F_{CH4}, the capture (drain) occurred during both periods at Nf (−26 and −79 $\mu\text{g C-CH}_4 \text{ m}^{-2} \text{ h}^{-1}$) as well as Ti and Th (−21 and 12 $\mu\text{g C-CH}_4 \text{ m}^{-2} \text{ h}^{-1}$, respectively). F_{N2O} also presented low values during both periods and showed a tendency to drain N₂O from the atmosphere, especially at Nf (−2 $\mu\text{g N-N}_2\text{O m}^{-2} \text{ h}^{-1}$). In addition, F_{N2O} was slightly positive for Ti and Th (0.3 and 0.55 $\mu\text{g N-N}_2\text{O m}^{-2} \text{ h}^{-1}$, respectively). Soil moisture did not show a correlation ($p > 0.05$) with the measured greenhouse gas fluxes. A scenario of increased temperatures

* Corresponding author.

E-mail address: alan.panosso@unesp.br (A.R. Panosso).

might result in changes in the balance between the emissions and drains of these gases from soils, leading to higher emission values of CH_4 and N_2O , especially for tundra covered soils (Ti and Th), where the highest average fluxes and thermohydric variations were observed over the year.

© 2018 Elsevier B.V. All rights reserved.

1. Introduction

Global warming and the increased emissions and concentrations of greenhouse gases (GHG) in the atmosphere have been a recurring theme in scientific papers since the last decade (Batjes, 1996; Blagodatsky and Smith, 2012). Soils are primarily responsible for the production and consumption of atmospheric GHG and have been directly related to global climate change. Among GHGs, carbon dioxide (CO_2), nitrous oxide (N_2O), and methane (CH_4) are the most impactful (IPCC, 2007).

Soils are one of the largest GHG reservoirs and play an important role in the biogeochemical cycles of carbon and nitrogen on Earth (IPCC, 2007). Studies have indicated that soils from natural environments of undisturbed ecosystems may become large sources of or drains of GHG due to the likely global increase in average annual temperatures (Butterbach-Bahl et al., 2002; Smith et al., 2008). This situation is relatively well known for northern hemisphere soils since most of the polar and sub-polar soils have large carbon stocks preserved by low temperatures, and especially by the permafrost (Michaelson et al., 2004; Michel et al., 2006; Simas et al., 2008). As a result, these soils have been considered potential sources of GHG emissions to the atmosphere (Michaelson et al., 2004; Oechel and Billings, 1992; IPCC, 2007; Thomazini et al., 2015, 2016; Pires et al., 2017).

Currently, 60% of the terrestrial surface on Earth experiences seasonal snow cover or soil freezing (Brooks et al., 2011). These phenomena occur particularly at high latitudes, where more than half of the soil carbon is stocked (Post et al., 1982). In these regions, low temperatures and primary productivity preserve carbon and other nutrients, delaying soil organic matter decomposition (Callaghan and Jonasson, 1995). In the Southern Hemisphere, especially in South America, few studies have been conducted on soils and periglacial environments, except for studies of the Maritime Antarctic (Blume et al., 2002; Beyer, 2004; Michel et al., 2006; Simas et al., 2007, 2008). In this context, the potential impacts of global climate change on these environments are not well known.

High-latitude regions are very sensitive to global climate change due to soil temperatures near the freezing point of water (IPCC, 2007). Thus, small changes in temperature may be sufficient to modify the region's peculiar thermal dynamics (snow cover, seasonal freezing, and freeze-thaw cycles). An increase of 1 to 4 °C in the annual average air temperature is projected for latitudes ranging from 30 to 55° S, depending on the scenario considered (Magrin et al., 2014).

The deciduous forests of *Nothofagus* spp. and tundra environments found in Tierra del Fuego are natural environments that have been altered little by humans (Strelin and Iturraspe, 2007), with appropriate characteristics to obtain reference values for the Southern Hemisphere's highland environments. Studies on in situ measurements may contribute to constructing models and projecting future scenarios on global warming effects that are closer to reality. The hypothesis of our study is that increasing soil temperature and moisture will result in GHG fluxes changes, especially during the summer period, at the different vegetation patterns in Patagonia region. Thus, the aim of this study was to assess F_{CO_2} , $F_{\text{N}_2\text{O}}$, and F_{CH_4} at sites of *Nothofagus* forest and tundra-covered soils of the Martial Valley, Darwin Cordillera, during two periods, i.e., at the beginning of glacier thaw (spring) and the height of summer, in order to assess temperature and moisture effects on GHG fluxes. These fluxes were correlated with chemical, physical, and climatic attributes, allowing comparison with soils from other natural environments.

2. Materials and methods

2.1. Location and characterization of sampling sites

GHG sampling was performed in the Martial Sur sector (Strelin and Iturraspe, 2007) of the Martial glacier, Tierra del Fuego, Ushuaia, Argentina, with geographical coordinates 54°47'39.7" S and 68°23'42.8" W (Fig. 1). The Martial glacier is one of the glacial circuses of the Darwin Cordillera in the extreme south of the Andes (Strelin and Iturraspe, 2007). The regional climate is cold oceanic, with strong southwest winds in late spring and early summer (Tuhkanen, 1992). The average annual temperature at Ushuaia is 5.5 °C, with an average temperature of 1.6 °C in the coldest month (July) and 9.6 °C in the warmest month (January) (Puigdefábregas et al., 1988). Soils have a cryic temperature regime, in which the average annual soil temperature at 0.50 m is below 8 °C but above 0 °C and in which the variation between summer and winter months is lower than 6 °C (Soil Survey Staff, 2014). At 600 m above sea level, the estimated average annual temperature is 2.5 °C; at 900 m, where the cold polar climate occurs, it is close to 0 °C (Puigdefábregas et al., 1988).

The experimental sites were divided as follows. **Nf** is an area at the upper limit of the forest, with vegetation of *Nothofagus pumilio* and *Nothofagus antarctica* in the lowest position on the hillside (altitude of 600 m), a steep slope (45°) and good drainage conditions. The area is one of the oldest moraines of glacier retreat and presents soil texture that is slightly more clayey than that of the other studied sites. The surface horizon is moderate and shallow, and the soils do not freeze in the winter. The **Ti** area is at the beginning of tundra colonization, with vegetation, with high species variability, mainly composed by cushion plants of *Bolax gummifera* (Apiaceae) also known as yareta, one of the most characteristic plants in the Martial Mountains and *Empetrum rubrum* (Empetraceae), a prostrate shrub, these being accompanied by mosses and lichens, in an intermediate position on the hillside (altitude of 660 m), a steep slope (40°) and good drainage conditions (moderately drained). Cushion vegetation is discontinuous and covers approximately 50% of the soil surface with a moderate and shallow surface horizon. Soils have a freezing front up to 0.30 m during 4 to 6 months in the winter, depending on the depth considered. The **Th** area is at the highest part of the hillside (altitude of 770 m), with a well-developed tundra vegetation composed of *Bolax gummifera* and *Empetrum rubrum* and a lower slope close to the drainage line (35°). Cushion vegetation covers the entire soil surface, forming a slightly thick organic horizon. During the summer, soil waterlogging is intense, and the thaw water flows superficially (imperfectly drained). In these soils, the freezing front reaches 0.50 m and is extended for 4 to 6 months.

Soils of these three sites were classified as Inceptisols by soil taxonomy. A soil profile was described and sampled at each of the three measurement sites. Chemical and physical analyses were carried out following the standard procedures of EMBRAPA (1997). Textural fractionation was performed using 0.1 M NaOH as a dispersant and stirring with slow rotation for 16 h (EMBRAPA, 1997). Soil bulk density was obtained by the volumetric ring method, and samples were collected in triplicate (EMBRAPA, 1997). The calculated carbon stock was corrected for the fraction higher than 0.5 mm, which was determined by sieving the soil samples. The following equation was used to calculate the carbon stock according to Eq. (1) (Batjes, 1996):

$$\text{Cst} = (\text{TOC}) \times (\text{Ds}) \times (\text{SLT}) \times (1 - \% \text{fragments} > 0.5 \text{ mm}) \quad (1)$$

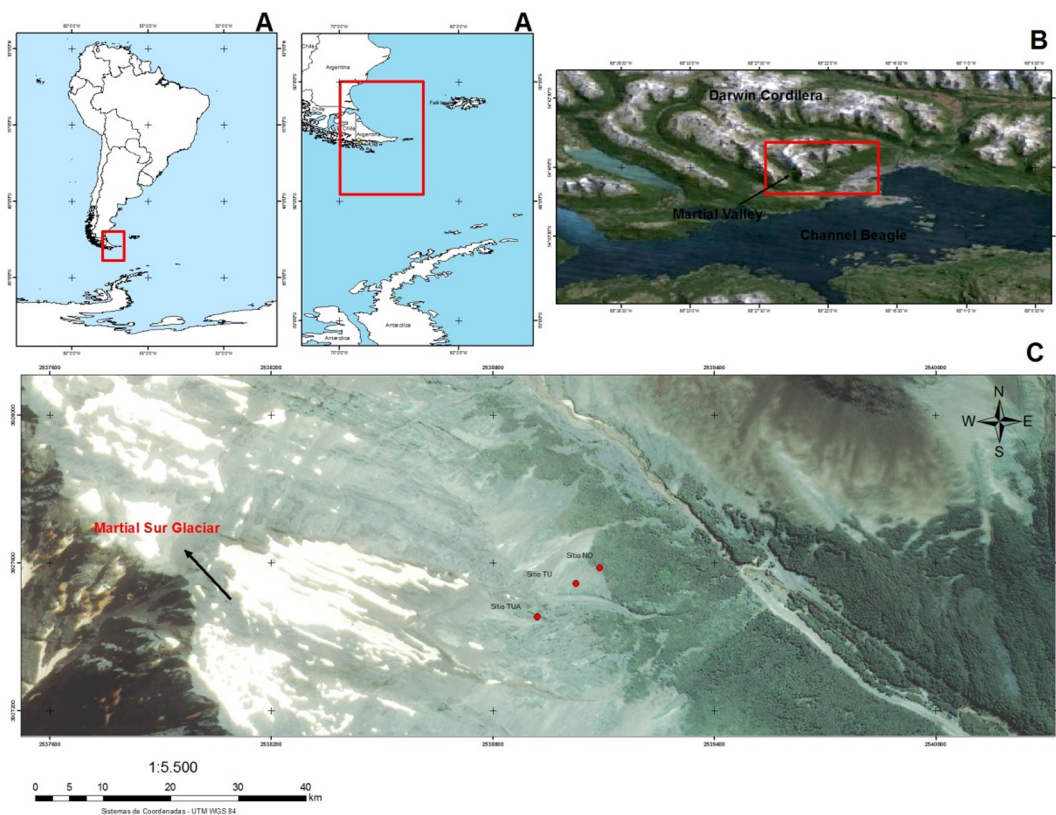


Fig. 1. Location of the study area. A) Tierra del Fuego in South America; B) Martial Glacier Valley, Darwin Cordillera; C) Location of the study sites.

where C_{st} is the carbon stock ($Mg\ m^{-2}$), TOC is the total organic carbon ($g\ C\ g^{-1}$ soil), D_s is the soil bulk density ($Mg\ m^{-3}$), and SLT is the soil layer thickness (m).

The exchangeable cations Ca^{+2} , Mg^{+2} , and Al^{+3} were extracted with 1 M KCl solution and measured with an atomic absorption spectrophotometer. K^+ , Na^+ , and available P were extracted with the Mehlich 1 method ($0.05\ M\ HCl + 0.0125\ M\ H_2SO_4$) and measured by a spectrophotometer (available P) and flame emission photometer (Na^+ and K^+) (EMBRAPA, 1997). Potential acidity ($H^+ + Al^{+3}$) was determined by titration after extraction with $0.5\ mol\ L^{-1}$ Ca (CH_3COO_2) at pH 7.0. Soil pH was measured in distilled water and 1 mol L^{-1} KCl solution (EMBRAPA, 1997). Organic matter content determination by the muffle method was performed according to Goldin (1987) with the following modifications: samples were dried in an oven at $105\ ^\circ C$ for 24 h to eliminate all water from the residues, such as the hygroscopic, capillary, or crystallization water (Rodella and Alcarde, 1994). After this period, ceramic crucibles with samples were placed in a muffle oven and incinerated at a temperature of $550\ ^\circ C$ for 3 h. Subsequently, the set crucibles + residues were placed in a desiccator and then weighed (EMBRAPA, 1997). Total nitrogen (TN) was determined by the Kjeldahl method (EMBRAPA, 1997). Soils were classified according to the criteria adopted by the soil taxonomy classification system (Soil Survey Staff, 2014) (Table 2).

The methodology used for ammonium measurements was salicylate colorimetry, which is based on the formation of an emerald blue complex when NH_3 and salicylate react in the presence of NaOCl at high pH conditions, with sodium nitroprusside as a catalyst (Kempers and Zweers, 1986). Nitrate was measured via two-wavelength ultraviolet spectrometry; the absorbance reading at 210 nm comprises the sum of nitrate and impurities, and the reading at 275 nm comprises only impurities. The difference between both readings is the nitrate-associated absorbance (Miyazawa et al., 1985).

2.2. CO_2 , CH_4 , and N_2O emissions

At each of the three sites, six points were circularly distributed around the site of soil description for sampling F_{CH_4} and F_{N_2O} (chambers) and F_{CO_2} (collars) (Fig. 2). Campbell CR1000 data logger devices (Campbell Scientific Inc.), equipped with sensors for measuring soil and air temperature at depths of 5, 10, 30, 50, and 100 cm (model 105E and 107 Temperature Probe) and soil moisture at depths of 10, 30, 50, and 100 cm (model CS616-L), were installed in the profile of each site.

Previous soil temperature (T_s) data from each site were used to identify the time at which the average hourly temperature of the sampling month occurs between 12 and 15 h local time. Two measurements

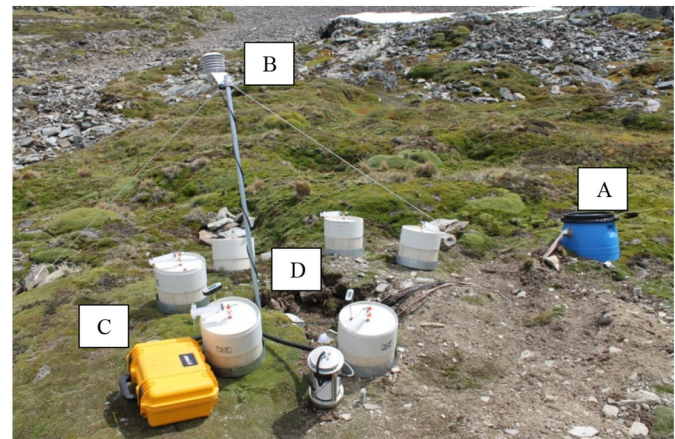


Fig. 2. Sampling scheme used at the highest environment (Th). A) Storage devices of soil temperature and moisture; B) Air temperature sensor suspended by a metal rod; C) LI-8100 system used for sampling CO_2 flux; D) Six PVC chambers for sampling N_2O and CH_4 .

were performed at each site (Nf, Ti, and Th). The first measurement corresponded to the period between November 29 and December 5, 2011, at the onset of soil defrost, with lower temperatures and higher soil moisture. The second measurement corresponded to the period between February 1 and 6, 2012, during the summer season, with high temperatures and lower soil moisture. For each period, daily samplings were performed at the same time.

Soil CO₂ flux (F_{CO_2}) was measured by an LI-8100 system (LI-COR Biosciences, USA, Fig. 2C) coupled to PVC collars installed at each site. This system monitors changes in CO₂ concentration inside the chamber via spectroscopy in the infrared region (IRGA, Infrared Gas Analyzer). The chamber is a closed system (internal volume of 854.2 cm³) with a soil contact area of 83.7 cm². Six PVC collars were installed around each profile, and three cycles of consecutive readings were performed for each collar, totaling 288 measurements per period and 576 measurements in total. During each measurement, the apparatus performed an initial 30-s cycle to stabilize the airflow inside the chamber, followed by 90 s of flux measurement. CO₂ fluxes were expressed in µg m⁻² s⁻¹. Together with CO₂ flux measurements, soil temperature was measured using a thermometer (Delt DT-625N).

F_{N_2O} and F_{CH_4} were measured using six chambers of polyvinyl chloride (PVC) fixed to the soil by galvanized steel bases with dimensions of 0.25 × 0.20 m, inserted into the soil to a depth of 0.05 m (Fig. 2D). The seal between the chamber and base was made of insulating rubber. Each PVC chamber was composed of a hole for inserting a three-way valve (Discofix B BRAUN) and another for fixing a thermometer (model Delt DT-625 N), both sealed by insulating rubber. The Discofix valve allowed for sealing and guiding gas exhaust from the chamber into a vial at the sampling time. Before gas sampling, vials were pressure-primed by a manual pump for internal air removal. Samplings were performed in each chamber at 0, 20, 40, and 60 min after closure and reopened after this procedure. In each period, 432 gas samplings were performed, totaling 864 samples of CH₄ and N₂O. At each site, ambient air samples were collected for gas flux calculation, totaling 36 samples.

N₂O concentration analysis was performed using a gas chromatograph (Perkin Elmer, Autosystem) equipped with a Porapak Q column and an electron capture detector. Before each analysis, standards were injected to calculate the N₂O concentrations of each sample. The standards used were 482, 800, and 1180 ppbv N₂O. N₂O fluxes (F_{N_2O}) are the difference between the concentrations of each treatment sample and ambient air sample, calculated as Eq. (2):

$$FN_2O = \frac{dC}{ct} \left(\frac{V}{A} \right) \frac{M}{Vm} \quad (2)$$

where dC/dt is the change in N₂O concentration in the chamber at the incubation interval, V is the chamber volume, A is the soil area covered by the chamber, M is the molecular weight of N₂O, and V_m is the molecular volume at the sampling temperature. Fluxes were expressed in µg N-N₂O m⁻² h⁻¹. After flux calculation, the emissions for the studied time interval were estimated. This same method was used to estimate CH₄ fluxes.

2.3. Statistical analyses

Descriptive statistics were used to obtain the mean, standard deviation, coefficient of variation, minimum, and maximum values of F_{CO_2} , F_{N_2O} , and F_{CH_4} . For temperature (air and soil) and soil moisture, the mean, minimum, and maximum values were calculated. The results were subjected to analysis of variance by means of the Snedecor's F test at the 5% significance level. Discarding the null hypothesis, the differences between means were tested by Tukey's test at the 5% significance level. The association between gas fluxes and environmental variables (temperature and moisture) was tested by Pearson's linear

correlation analysis at a 5% significance level using the software XLSTAT 7.5 (ADINSOFT, 2004).

3. Results

3.1. Soil temperature and moisture

During the study periods, soil temperature remained above 0 °C, and the effects of freezing and thawing on GHG emissions were excluded. However, a strong climatic variation was observed during the experimental period. In the first sampling period, the soil temperature at a depth of 0.05 m varied from 1.7 to 13.6 °C at the three sites, with lower temperatures on the first two sampling days and higher temperatures on the fourth and fifth days (Fig. 3). On the first and second sampling days, temperatures remained lower due to snow precipitation, which caused a thick accumulation of snow on the sites. On the third, fourth, and fifth sampling days, the soil temperature increased due to a higher incidence of solar radiation (sunny days) and the absence of precipitation. On the penultimate sampling day, the temperature dropped due to snow precipitation and strong winds. The highest temperature averages were obtained at Ti (8.2 °C) and Th (8.6 °C) when compared to Nf (4.56 °C) ($p < 0.05$). Both Ti and Th presented very similar thermal behavior, with values between 1 and 14 °C. For Nf, the thermal amplitude varied from 1.9 to 7 °C.

The soil temperature varied from 1.5 °C (on the fourth sampling day) to 13 °C (on the first and last day) during the second sampling period. On the first day, temperatures showed higher values, since this day was sunny and without snow or rain. On the second sampling day, temperatures started dropping, and the lowest values were obtained on the fourth sampling day (February 6, 2012), when strong snow precipitation was observed. On the fifth day, temperatures increased and reached their maximum values on the sixth day, when the day was sunny. On the last day, temperatures dropped again due to cloudy weather with strong winds, but without rain or snow. The three sites presented a similar thermal pattern but with temperatures lower than those during the previous period. Nf presented lower average temperatures (4.1 °C) and a lower amplitude of temperature variation over the sampling period (1.7 to 5.7 °C) when compared to the soils in tundra (Th and Ti), which presented higher average temperatures (8.5 and 7.7 °C, respectively), as well as a higher thermal amplitude ($p < 0.05$).

Considering the three sites, soil moisture (Ms) ranged from 0.093 to 0.195 m³ m⁻³ during the first period (Fig. 3). In this period, Nf and Ti presented small changes in soil moisture (0.161 to 0.195 m³ m⁻³), being more humid ($p < 0.05$) than Th at the beginning of the experiment. The water from glacier thaw increased the soil moisture from 0.093 to 0.195 m³ m⁻³ at Th, which was the most humid site on the last day (0.195 m³ m⁻³).

During the second sampling period, soil moisture ranged from 0.111 to 0.270 m³ m⁻³. Th presented the highest moisture and the highest variation of this variable during this period, reaching maximum values on the fifth day (February 7, 2012), soon after a heavy rain precipitation that occurred the day before. The Ms values at Nf and Ti were lower than those found in the first period (0.118 and 0.137 m³ m⁻³, respectively), with Ti slightly more humid than Nf. In general, the three sites presented good drainage conditions during the experimental period. Th presented Ms values slightly higher in the second sampling period but not high enough for soil saturation.

3.2. General properties of soils

The soil pH ranged from 4.8 to 5.3 for Th and Nf, respectively (Table 1). The clay content was similar at the studied sites (12 to 21 dag kg⁻¹), suggesting that the textural differences between sites interfere little with gas emissions. In the surface horizon, the soil density was lower at Th (0.19 g cm⁻³) and higher at Nf (0.60 g cm⁻³). The highest cation exchange capacity (CEC) value was observed at Ti,

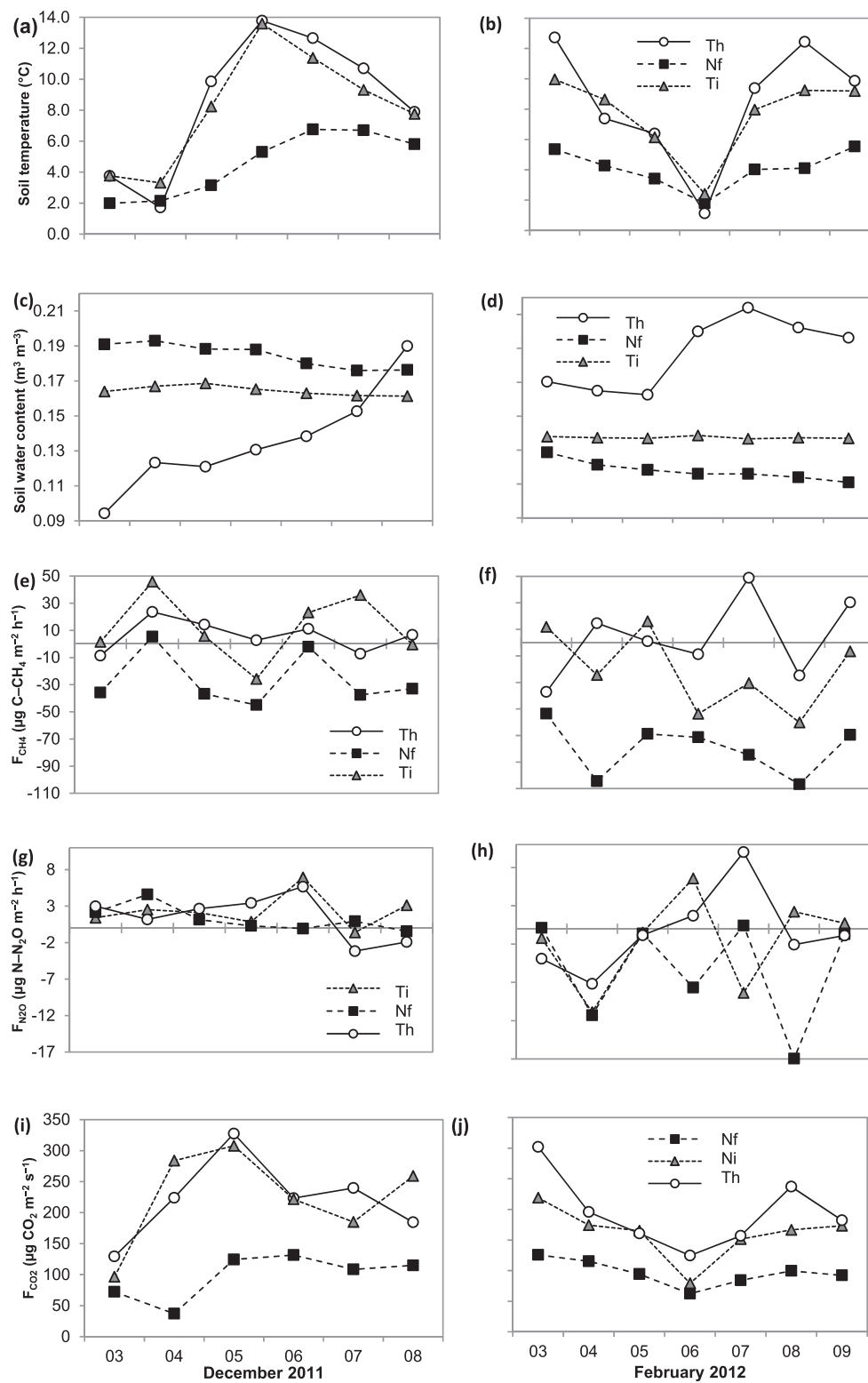


Fig. 3. Soil temperature at a depth of 2 cm (a) and (b), soil moisture at a depth of 10 cm (c) and (d), and daily average GHG fluxes (e-j) during the first and second sampling periods.

whereas the lowest value was found at Th. The sum of bases between sites was very similar, with values of 4.4 and 5.0 cmol_c kg⁻¹ at Nf and Th, respectively.

The distribution of soil organic C and N was different for each site, with the highest TOC contents in the surface horizon of Th (30 dag kg⁻¹) when compared to the other sites. However, the C stock was higher at Nf (Table 2). Th and Nf presented similar N

contents (approximately 1 dag kg⁻¹), whereas Ti presented the lowest contents of N (0.2 dag kg⁻¹) and TOC (7 dag kg⁻¹). The C/N ratio varied from 16 to 33 in the surface horizon of Nf and Ti, respectively. The nitrate contents were low and varied from 0.15 to 0.56 mg N- $\text{NO}_3^- \text{ g}^{-1}$ soil for Ti and Nf, respectively, whereas Th presented slightly higher contents (0.31 mg N- $\text{NO}_3^- \text{ g}^{-1}$ soil) than did Ti. Ammonium values were higher and ranged from 5.02 to 16.04 mg N-

Table 1

Soil chemical attributes and particle size distribution of the studied sites.

Hor.	Depth	pH	pH	SB cmol _c kg ⁻¹	CEC	TOC --- dag kg ⁻¹ ---	total N	C/N ¹	Sand ²	Silt ³	Clay ⁴	Ds ⁵	Cst ⁶ Mg m ⁻²
		cm	H ₂ O						----- g cm ⁻³ -----				
Nf – Andic Humicryods, <i>Nothofagus</i> forest, clay loam texture, well drained													
Oi	8–0	5.31	4.44	4.42	15.12	16.50	1.01	16.3	–	–	–	0.60	0.67
Bi	0–27	4.79	3.90	0.57	17.27	6.96	0.26	26.8	57	23	20	0.90	1.10
BC	27–55	5.45	4.33	2.11	15.81	3.48	0.20	17.4	62	20	18	1.20	0.18
Ti – Andic Humicrypts, tundra vegetation, clay loam texture, moderately drained													
A	0–15	5.16	3.88	4.40	21.20	7.58	0.23	33.0	59	24	17	0.34	0.33
Bi	15–40	5.54	4.19	2.53	15.93	4.69	0.21	22.3	64	19	17	0.88	0.67
BC	40–60	5.73	4.35	1.74	11.14	4.03	0.13	31.0	71	15	14	0.96	0.12
C	60–80	6.12	4.61	1.23	4.03	1.29	0.05	25.8	74	14	12	1.19	0.05
Th – Andic Dystrocrypts, tundra vegetation, loam texture, imperfectly drained													
Oi	12–0	4.81	3.91	5.03	10.53	30.40	0.97	31.3	–	–	–	0.19	0.59
A	0–18	4.85	3.75	4.12	21.42	15.84	0.60	26.4	57	23	20	0.23	0.43
Bi	18–30	5.60	4.03	4.19	14.89	3.69	0.20	18.5	45	35	20	0.99	0.22
BC	30–60	5.81	4.46	2.82	12.42	3.50	0.20	17.5	48	31	21	1.09	0.40
C	60–80	6.11	5.11	3.88	10.78	4.90	0.18	27.2	58	23	19	1.21	0.36

¹ Total organic carbon to total nitrogen ratio.² Coarse sand + fine sand fraction (0.05–2 mm).³ Silt fraction (0.002–0.05 mm).⁴ Clay fraction (<0.002 mm).⁵ Soil bulk density.⁶ Soil carbon stock.

NH_4^+ g⁻¹ soil for Th and Nf, respectively, whereas Ti presented a value of 9.93 mg N-NH₄⁺ g⁻¹ soil.

3.3. Soil CO_2 fluxes

F_{CO_2} ranged from 8.8 to 728.20 $\mu\text{g CO}_2 \text{ m}^{-2} \text{ s}^{-1}$ at the three sites, with an average flux of 181.77 $\mu\text{g CO}_2 \text{ m}^{-2} \text{ s}^{-1}$ for the first sampling period (Table 2 and Fig. 3). The lowest daily average values were observed for Nf (37.13 $\mu\text{g CO}_2 \text{ m}^{-2} \text{ s}^{-1}$) and the highest for Th (327.51 $\mu\text{g CO}_2 \text{ m}^{-2} \text{ s}^{-1}$). The highest F_{CO_2} values were observed on the fourth and fifth sampling days (December 2 and 3, 2011, respectively), coinciding with the days when the highest temperatures occurred ($r^2 = 0.85$). Th and Ti presented the highest F_{CO_2} values and a similar flux pattern with each other, with an average value of 223.56 $\mu\text{g CO}_2 \text{ m}^{-2} \text{ s}^{-1}$. On the other hand, Nf presented the lowest F_{CO_2} values, approximately 45% less than those of Th and Ti (Fig. 3).

During the second sampling period, the F_{CO_2} of the three sites ranged from 4.84 $\mu\text{g CO}_2 \text{ m}^{-2} \text{ s}^{-1}$ (Ti) to 453.05 $\mu\text{g CO}_2 \text{ m}^{-2} \text{ s}^{-1}$ (Th), with an average flux of 150.66 $\mu\text{g CO}_2 \text{ m}^{-2} \text{ s}^{-1}$ for the period. The lowest daily average values were observed for Nf (62.39 $\mu\text{g CO}_2 \text{ m}^{-2} \text{ s}^{-1}$), whereas the highest values were found at Th (302.16 $\mu\text{g CO}_2 \text{ m}^{-2} \text{ s}^{-1}$). On the first sampling day, a higher average flux was observed at all sites, with Th presenting the highest values and an average flux of 302.16 $\mu\text{g CO}_2 \text{ m}^{-2} \text{ s}^{-1}$ (the day with the highest soil temperature) ($r^2 = 0.89$). In contrast, the lowest emissions occurred on the day with lower soil

temperatures (February 6, 2012). During this period, F_{CO_2} was approximately 100% higher at Th than at Nf, with an average value of 194.4 $\mu\text{g CO}_2 \text{ m}^{-2} \text{ s}^{-1}$.

3.4. Soil CH_4 fluxes

During the first sampling period, F_{CH_4} ranged from -204.6 to 208.3 $\mu\text{g C-CH}_4 \text{ m}^{-2} \text{ h}^{-1}$, with an average value of -2.66 $\mu\text{g C-CH}_4 \text{ m}^{-2} \text{ h}^{-1}$, where negative and positive values indicate absorption and net flux of CH_4 from the soil to the atmosphere, respectively. The highest daily average flux was observed at Ti (45.88 $\mu\text{g C-CH}_4 \text{ m}^{-2} \text{ h}^{-1}$), whereas the lowest flux was observed at Nf (-44.95 $\mu\text{g C-CH}_4 \text{ m}^{-2} \text{ h}^{-1}$). The average fluxes found at Nf presented low and negative values. The highest average flux values occurred on the first day, which was the only day that presented positive flux at the three sites (Table 2 and Fig. 3) ($r^2 = -0.36$).

Considering the three sites, F_{CH_4} ranged from -198 to 193 $\mu\text{g C-CH}_4 \text{ m}^{-2} \text{ h}^{-1}$ during the second sampling period, with an average flux of -32.43 $\mu\text{g C-CH}_4 \text{ m}^{-2} \text{ h}^{-1}$. As in the first sampling period, tundra sites presented higher F_{CH_4} values. However, compared to Ti, Th presented the highest emission values during the second sampling period. The highest daily average flux values of Th (48.9 $\mu\text{g C-CH}_4 \text{ m}^{-2} \text{ h}^{-1}$) were obtained on the fifth day (February 7, 2012), coinciding with the day of higher soil moisture ($r^2 = 0.72$) (Table 2 and Fig. 3).

Table 2Descriptive statistics for CO_2 , CH_4 , N_2O emissions, Ts and Ms at the studied sites.

Period	F_{CO_2} ($\mu\text{g CO}_2 \text{ m}^{-2} \text{ s}^{-1}$)		F_{CH_4} ($\mu\text{g C-CH}_4 \text{ m}^{-2} \text{ h}^{-1}$)		$F_{\text{N}_2\text{O}}$ ($\mu\text{g N-N}_2\text{O} \text{ m}^{-2} \text{ h}^{-1}$)		Ts (°C)		Ms ($\text{m}^3 \text{ m}^{-3}$)	
	Min/Max	Mean ± SE	Min/Max	Mean ± SE	Min-Max	Mean ± SE	Min/Max	Mean	Min/Max	Mean
NO										
Dec. 2011	8.8/261.65	98.17 ± 14.83	-121.2/61.8	-26.4 ± 8.8	-16/16.9	1.2 ± 0.7	1.9/7.0	4.6	0.176/0.195	0.185
Feb. 2012	20.39/220.55	96.33 ± 9.24	-198.1/116.2	-79.8 ± 8.8	-29.9/38.3	-5.2 ± 2.8	1.7/5.7	4.1	0.111/0.129	0.118
TU										
Dec. 2011	50.16/728.20	225.72 ± 31.42	-128.2/208.3	12.3 ± 10	-9.3/13.6	2.3 ± 1	2.6/14.8	8.2	0.161/0.169	0.164
Feb. 2012	4.84/408.76	161.38 ± 17.08	-144.7/101.3	-21 ± 12.2	-24.5/27.6	-1.7 ± 2.5	2.0/10.8	7.7	0.136/0.139	0.137
TUA										
Dec. 2011	32.71/662.64	221.41 ± 26.73	-204.6/126.8	6.1 ± 4.7	-11.0/8.6	1.6 ± 1.4	1.3/14.7	8.6	0.093/0.195	0.136
Feb. 2012	40.92/453.05	194.4 ± 24.15	-151.9/193.9	3.5 ± 12.4	-34.4/30.6	-0.5 ± 2.2	0.5/13.9	8.5	0.162/0.270	0.187

Min = minimum; Max = maximum; SE = standard error of the mean.

3.5. Soil N_2O fluxes

In the first sampling period, F_{N2O} ranged from -16.04 to $16.90 \mu\text{g N-N}_2\text{O m}^{-2} \text{h}^{-1}$, with an average value of $1.71 \mu\text{g N-N}_2\text{O m}^{-2} \text{h}^{-1}$. The lowest average value was observed at Nf ($1.55 \mu\text{g N-N}_2\text{O m}^{-2} \text{h}^{-1}$), whereas the highest value was found at Ti ($2.33 \mu\text{g N-N}_2\text{O m}^{-2} \text{h}^{-1}$) (Fig. 3). F_{N2O} fluxes were often low ($<5 \mu\text{g N-N}_2\text{O m}^{-2} \text{h}^{-1}$) but positive. The highest daily average flux values were observed at Ti ($6.94 \mu\text{g N-N}_2\text{O m}^{-2} \text{h}^{-1}$) and Th ($5.66 \mu\text{g N-N}_2\text{O m}^{-2} \text{h}^{-1}$) on the fifth sampling day, which was the day after the highest soil temperature.

Furthermore, in the summer period, F_{N2O} values ranged from -34.4 to $38.3 \mu\text{g N-N}_2\text{O m}^{-2} \text{h}^{-1}$, with a negative average flux of $-2.4 \mu\text{g N-N}_2\text{O m}^{-2} \text{h}^{-1}$ (Table 2 and Fig. 3). The average fluxes were lower for Nf ($-5.2 \mu\text{g N-N}_2\text{O m}^{-2} \text{h}^{-1}$) and higher for Th ($-0.5 \mu\text{g N-N}_2\text{O m}^{-2} \text{h}^{-1}$). The highest daily average emission occurred at Th ($10 \mu\text{g N-N}_2\text{O m}^{-2} \text{h}^{-1}$) and coincided with the day with higher soil moisture and temperature (Fig. 5).

4. Discussion

4.1. Organic matter and mineral N in soil profiles

The C and N contents in Nothofagus forest soil were similar to those reported in the literature for other soils of Tierra del Fuego and the Patagonia mountainous region (Peri et al., 2013). Frangi et al. (2005) reported that soil organic matter (SOM) of Nothofagus temperate forests presents a high C concentration and C/N ratio (approximately 37), with low N concentrations, being those values higher than the ones observed in forest soils of our study. For tundra-covered soils of the Tierra del Fuego, little data can be found in the literature regarding soil C and N contents. The TOC contents in the organic horizons of Th were higher among the three sites, and it is believed that a higher C content is related to a higher soil moisture ($r^2 = 0.93$). However, the C/N ratio at the tundra sites (Th + Ti) was higher than the values found in forest soils.

Ammonium values were higher for all sites when compared to nitrate values, indicating a restriction in the nitrification process due to the low moisture found in these soils. According to Gregorich et al. (2006), elevated ammonium contents in relation to soil nitrate indicate the occurrence of biological mineralization of organic N. However, low nitrate contents suggest a restriction of the nitrification process or, alternatively, that N-NO_3^- was lost by denitrification and/or leaching. The results indicate that at Nf, nitrate and ammonium concentrations were higher, suggesting that the SOM mineralization rate is faster in these soils. In this soil, the C/N ratio of SOM is closer to the microbial C/N ratio, and the SOM can be broken down with a lower energy expenditure when compared to tundra-covered soils (Ti + Th), which presented a higher C/N ratio.

4.2. Mineralization of organic matter and F_{CO2}

F_{CO2} values represent the respiratory activity of soil organisms (autotrophic and heterotrophic), which are affected by soil temperature (O'Neill et al., 2002; Stoffel et al., 2010; Olajuyigbe et al., 2012; Thomazini et al., 2016; Pires et al., 2017) and soil moisture (Schaufler et al., 2010; Stoffel et al., 2010), among other factors such as substrate availability, total N, and O₂. For our study, the daily CO₂ fluxes of the three sites presented a positive and significant correlation with soil temperature ($r > 0.74$, $p < 0.05$). However, no correlation was observed between Ms. and F_{CO2} ($p > 0.05$). The average F_{CO2} in both periods was low (132 and $174 \mu\text{g CO}_2 \text{m}^{-2} \text{s}^{-1}$), being lower in the second period due to the lower temperatures. These results indicate a possible increase in F_{CO2} in these areas due to a probable average increase in average global temperatures. Initially, this increase in F_{CO2} could lead to labile SOM consumption, reducing the humification process. However, due to the increase in the photosynthetic rate of plants, a higher contribution of SOM should occur, which may lead to an increase in SOM. The balance

of these processes will be responsible for defining these future ecosystem conditions.

Considering both periods, Ti and Th presented relatively high F_{CO2} values, with an average value of $177.89 \mu\text{g CO}_2 \text{m}^{-2} \text{s}^{-1}$ and a maximum value of $453.05 \mu\text{g CO}_2 \text{m}^{-2} \text{s}^{-1}$. Nf presented a distinct pattern for F_{CO2} in relation to tundra sites in both periods, showing average fluxes that were at least 84% lower than those found at Th and Ti. This is probably due to the lower soil temperature in the forest. The direct exposure of tundra in association with the higher position on the hillside makes the tundra sites more susceptible to climatic conditions, further heating the soils. In addition, forest canopy favors the occurrence of lower and milder temperatures, which results in lower CO₂ emissions (Fig. 3).

When compared to most of the Maritime Antarctic soils (44 to $132 \mu\text{g CO}_2 \text{m}^{-2} \text{s}^{-1}$), the F_{CO2} registered in our study was higher (Orchard and Corderoy, 1983). On the other hand, the F_{CO2} values presented here were lower than the fluxes reported by Loureiro (2012) and Orchard and Corderoy (1983) for soils highly affected by ornithogenesis, whose biological activity is very high even at low temperatures (1–3 °C) due to the contribution of a high organic substrate that is easily decomposed (low C/N ratio). According to Loureiro (2012), in areas affected by Antarctic ornithogenic soils, sites where guano (excrements and bird remains) is concentrated present emissions approximately 100 times higher in relation to adjacent areas and at least 10 times higher than those at the sites of this study. Thomazini et al. (2015) studied soil CO₂-C and N₂O-N emissions across a glacier retreat chronosequence in Maritime Antarctica and observed an increase of 440% in F_{CO2} in the presence of vegetation (mixture of lichens, *Usnea* spp., *Sanionia uncinata* and *D. antarctica*), with an increase in F_{CO2} away from the glacier front.

4.3. Methanogenesis and CH₄ emissions

Nf presented a strong tendency to drain CH₄ from the atmosphere in both periods. Negative values of F_{CH4} were consistently observed at Nf in both periods (-26 and $-79 \mu\text{g C-CH}_4 \text{m}^{-2} \text{h}^{-1}$, respectively). These results indicate that the oxidation process overlaps CH₄ production, especially in these soils. Methane oxidation occurred over the assessed period, but in a cyclical way, with periods of higher and lower soil absorption. Even immediately after a high precipitation event, F_{CH4} was low ($5.3 \mu\text{g C-CH}_4 \text{m}^{-2} \text{h}^{-1}$, higher average flux value) at Nf, whereas in other profiles, the flux was higher, with 23.5 and $45.9 \mu\text{g C-CH}_4 \text{m}^{-2} \text{h}^{-1}$ at Th and Ti, respectively (first sampling period) (Fig. 3).

Ti and Th presented F_{CH4} temporal patterns similar to each other when compared to Nf, with higher emissions probably due to higher values of temperature and moisture. The daily average fluxes were frequently positive at these sites, as well as the average of each period (4 – $5 \mu\text{g C-CH}_4 \text{m}^{-2} \text{h}^{-1}$). However, their F_{CH4} values were low, indicating that the different types of plant formations on Monte Martial absorbed more CH₄ from the atmosphere than they emitted. These results indicate that the tundra ecosystem studied here could be considered a methane drain area at the regional level (Fig. 3).

In soil, CH₄ is mainly produced by methanogenic archaea in anaerobic conditions and is consumed in aerobic conditions by methanotrophic bacteria (Madigan et al., 2010). Therefore, F_{CH4} was primarily favored in anoxic conditions, such as in soils with high moisture or a shallow water table (Ullah, 2009; Gundersen et al., 2012). Other factors, such as N deposition, soil temperature, texture, soil pH, substrate availability, and vegetation age, may also interfere with soil CH₄ emissions (Butterbach-Bahl et al., 2002; Aronson et al., 2012; Dijkstra et al., 2012; Rowlings et al., 2013; Harrison-Kirk et al., 2013). Soils may present a cyclic and seasonal pattern in CH₄ oxidation rates throughout the year, with higher emission rates during the wetter period (Alves et al., 2006). According to Adamsen and King (1993), higher CH₄ emissions during the rainy season would be associated with methanogenic archaea activity due to the decreased partial pressure of O₂.

Methane consumption by dry soils is one of the main routes of CH₄ loss from the atmosphere to the soil and represents approximately 8% of atmospheric CH₄ drains (King, 1997). Well-drained forest soils are known to be large drains of atmospheric CH₄ (Steudler et al., 1996; Price et al., 2004; Dalal and Allen, 2008), incorporating C into the soil. Emissions from Nf soils were lower than those measured by Fritz et al. (2011) in high-latitude wetlands (Patagonia). These authors measured fluxes in *Sphagnum* spp. covered soils and observed F_{CH₄} close to zero (0 to 1 µg C–CH₄ m⁻² h⁻¹) due to the predominance of aerobic conditions in the rhizosphere. Aerated soils have the ability to absorb atmospheric CH₄ through the oxidation promoted by aerobic bacteria (methanotrophic) to obtain energy and C, using O₂ for the monooxygenase (MMO) enzyme, which is indispensable for the CH₄ oxidation process (Smith et al., 2003; Mosier et al., 2004).

4.4. Nitrification, denitrification, and N₂O emissions

The average values of F_{N₂O} were low at the three sites during both periods, being lower in the second sampling period. Considering the three sites, F_{N₂O} presented a high coefficient of variation, which explains the absence of correlation between its fluxes and Ts and Ms. The highest average fluxes occurred at sites with the highest moisture content (Th and Ti), whereas the lower fluxes occurred in soils with lower moisture (Nf). However, soils with higher moisture contents favor denitrification (Maag and Vinther, 1999), which is the main process responsible for F_{N₂O} at a global level (Alves et al., 2006). Nitrification and denitrification are processes that give rise to soil F_{N₂O}, and both processes are dependent on oxygen availability but in opposite conditions (Alves et al., 2006). Nitrification is the biological oxidation of reduced N forms, and the chemoautotrophic bacteria population is the main group responsible for this process (Killham, 1986). Because it is an aerobic process, nitrification is a pathway of NO₂, N₂O and NO₃ formation in well-drained soils (Poth and Focht, 1985). Therefore, nitrification was probably the predominant process of N₂O production in soils in this study due to the low moisture content for the denitrification process.

In addition to temperature and moisture, soil mineral N availability is another factor considered key for F_{N₂O} levels (Smith et al., 2003). Natural areas also present high fluxes, especially those where an N input and low C/N ratio can be found (ornithogenic soils in Antarctica) or in soils with high water content. In this study, the N₂O fluxes of the three sites were very low (−2.4 to 1.3 µg N–N₂O m⁻² h⁻¹), which is in accordance with the previously reported fluxes in natural areas with cold climates (Sun et al., 2002; Gregorich et al., 2006; Takakai et al., 2008; Kato et al., 2011). As observed by Smith et al. (2003), the microorganisms responsible for this process are dependent on SOM mineralization to make N available; if there is no considerable N addition, the amount of N available in the soil will be low.

Nitrification occurs when O₂ is available; however, when this gas is limited, denitrification occurs (Saggard et al., 2007; Pérez et al., 2000). The intensity of soil nitrate reduction depends mainly on soil O₂ concentrations. In these soils, good drainage conditions are predominant, and nitrate and ammonium contents of these soils corroborate the nitrification process. F_{N₂O} is the result of both production and consumption processes in the soil profile (Chapuis-Lardy et al., 2007). The data indicate a tendency of Nothofagus forest soils to work as a drain of N₂O from the atmosphere. This ecosystem can counterbalance other areas with high potential for greenhouse gas emissions. Some studies have reported the occurrence of soils that drain N₂O in different natural environments (Chapuis-Lardy et al., 2007). Furthermore, the soil pH of the most superficial layers of the three sites is likely very acidic, which favors nitrification, and at the same time, the low temperatures contribute to decreasing the denitrification process, which leads to a condition of almost nonsignificant F_{N₂O} (very close to zero).

5. Conclusions

This study provided the first in situ measurements of F_{CO₂}, F_{CH₄}, and F_{N₂O} in Nothofagus forest and tundra-covered soils in the region of Tierra del Fuego, Southern Patagonia. The data show a pattern of low fluxes for the three studied gases during the two periods. F_{CO₂} presented a high positive correlation with soil temperature. Soils covered with tundra presented the highest fluxes in relation to the forest soils. At the forest and tundra sites, a strong CH₄ capture by the soil (oxidation process) was observed in both periods, and a seasonal effect on CH₄ oxidation rates occurred, with a slight reduction during periods of higher soil moisture. CH₄ fluxes were higher in soils with high moisture. Furthermore, N₂O fluxes were very low in tundra and forest ecosystems. Forest soils may represent large drains of N₂O from the atmosphere in this region. On the other hand, tundra-covered soils present a greater environmental fragility due to a higher thermohydric amplitude and higher average values of GHG fluxes. Therefore, an increase in the average global temperatures could cause a greater effect on these soils, favoring higher GHG fluxes.

Acknowledgements

The authors would like to thank the following Brazilian institutions for their financial support: Brazilian Federal Agency for Support and Evaluation of Graduate Education (CAPES) and Brazilian National Council for Scientific and Technological Development (CNPq).

References

- Adamsen, A.P.S., King, G.M., 1993. Methane consumption in temperate and subarctic forest soils: rates, vertical zonation, and responses to water and nitrogen. *Appl. Environ. Microbiol.* 59, 485–490.
- ADINSOFT, 2004. XLSTAT-PLS 1.8. Statistical Software to MS Excel.
- Alves, B.J.R., Zottarelli, L., Fernandes, F.M., Heckler, J.C., Macedo, R.A.T.D., Boddey, R.M., Jantalia, C.P., Urquiza, S., 2006. Biological nitrogen fixation and nitrogen fertilizer on the nitrogen balance of soybean, maize and cotton. *Pesq. Agrop. Brasileira* 41, 449–456 [in Portuguese].
- Aronson, E.L., Vann, D.R., Heliiker, B.R., 2012. Methane flux response to nitrogen amendment in an upland pine forest soil and riparian zone. *J. Geophys. Res.* 117, G03012. <https://doi.org/10.1029/2012JG001962>.
- Batjes, N.H., 1996. Total carbon and nitrogen in the soils of the world. *Eur. J. Soil Sci.* 47, 151–163.
- Beyer, L., 2004. Ecological processes of Cryosols: introduction. In: Kimble, J. (Ed.), *Cryosols – Permafrost Affected Soils*. Springer-Verlag, Berlin, pp. 461–462.
- Blagodatsky, S., Smith, P., 2012. Soil physics meets soil biology: towards better mechanistic prediction of greenhouse gas emissions from soil. *Soil Biol. Biochem.* 47, 78–92. <https://doi.org/10.1016/j.soilbio.2011.12.015>.
- Blume, H.P., Beyer, L., Kalk, E., Kuhn, D., 2002. Weathering and soil formation. In: Böltner, L., Beyer e M. (Ed.), *Geocology of Antarctic Ice-free Coastal Landscapes*. Springer-Verlag, Berlin, pp. 114–138.
- Brooks, P., Grogan, P., Templer, P.H., Groffman, P., Oquist, M.G., Schimel, J., 2011. Carbon and nitrogen cycling in snow-covered environments. *Geogr. Compass* 5, 682–699.
- Butterbach-Bahl, K., Rothe, A., Papen, H., 2002. Plant and Soil. 240, p. 91. <https://doi.org/10.1023/A:101582701885>.
- Callaghan, T.V., Jonasson, S., 1995. Arctic terrestrial ecosystems and environmental change. *Philos. Trans. R. Soc. Lond.* 352, 259–276.
- Chapuis-Lardy, L., Wrage, N., Metay, A., Chotte, J., Bernoux, M., 2007. Soils, a Sink for N₂O? A review. *Glob. Chang. Biol.* 13, 1–17.
- Dalal, R.C., Allen, D.E., 2008. Greenhouse gas fluxes from natural ecosystems. *Aust. J. Bot.* 56, 369–407.
- Dijkstra, F.A., Pendall, E., Morgan, J.A., Blumenthal, D.M., Carrillo, Y., LeCain, D.R., Follett, R.F., Williams, D.G., 2012. Climate change alters stoichiometry of phosphorus and nitrogen in a semiarid grassland. *New Phytol.* 196, 807–815. <https://doi.org/10.1111/j.1469-8137.2012.04349.x>.
- EMBRAPA, 1997. *Centro Nacional de Pesquisa de Solos. Manual de métodos de análise de solo*, 2nd ed. Centro Nacional de Pesquisa de Solos, Rio de Janeiro (212 p.).
- Frangi, J.L., Barrera, M.D., Richter, L.L., Lugo, A.E., 2005. Nutrient cycling in Nothofagus pumilio forests along an altitudinal gradient in Tierra del Fuego, Argentina. *For. Ecol. Manag.* 217, 80–94.
- Fritz, C., Pancotto, V.A., Elzenga, J.T., Visser, E.J., Grootjans, A.P., Pol, A., Iturraspe, R., Roelofs, J.G., Smolders, A.J., 2011. Zero methane emission bogs: extreme rhizosphere oxygenation by cushion plants in Patagonia. *New Phytol.* 190, 398–408. <https://doi.org/10.1111/j.1469-8137.2010.03604.x>.
- Goldin, A., 1987. Reassessing the use of loss-on-ignition for estimating organic matter content in noncalcareous soils. *Commun. Soil Sci. Plant Anal.* 18, 1111–1116.

Gregorich, E.G., Beare, M.H., McKim, U.F., Skjemstad, J.O., 2006. Chemical and biological characteristics of physically uncomplexed organic matter. *Soil Sci. Soc. Am. J.* 7, 975–985.

Gundersen, P., Christiansen, J.R., Alberti, G., Brüggemann, N., Castaldi, S., Gasche, R., Kitzler, B., Klemedtson, L., Lobo-do-Vale, R., Moldan, F., Rütting, T., Schleppi, P., Weslien, P., Zechmeister-Boltenstern, S., 2012. The response of methane and nitrous oxide fluxes to forest change in Europe. *Biogeosciences* 9 (10), 3999–4012.

Harrison-Kirk, T., Beare, M.H., Meenken, E.D., Condron, L.M., 2013. Soil organic matter and texture affect responses to dry/wet cycles: effects on carbon dioxide and nitrous oxide emissions. *Soil Biol. Biochem.* 57, 43–55.

IPCC, 2007. Climate change 2007: the physical science basis. In: Solomon, S., Qin, D., Manning, M., Chen, Z., Marquis, M., Averyt, K.B., Tignor, M., Miller, H.L. (Eds.), Contribution of Working Group I to the Fourth Assessment Report of the Intergovernmental Panel on Climate Change. Cambridge University Press, Cambridge, United Kingdom and New York, NY, USA.

Kato, T., Hirota, M., Tang, Y.H., Wada, E., 2011. Spatial variability of CH₄ and N₂O fluxes in alpine ecosystems on the Qinghai-Tibetan Plateau. *Atmos. Environ.* 45, 5632e5639.

Kempers, A.J., Zweers, A., 1986. Ammonium determination in soil extracts by the salicylate method. *Soil Science Plant Analysis*. New York. v.17, n.7, pp. 715–723.

Killham, K., 1986. Heterotrophic nitrification. In: Prosser, J.I. (Ed.), *Nitrification*. IRL Press Oxford, United Kingdom, pp. 117–126.

King, G.M., 1997. Responses of atmospheric methane consumption by soils to global climate change. *Glob. Chang. Biol.* 3 (4), 351–362. <https://doi.org/10.1046/j.1365-2486.1997.00090.x>.

Loureiro, D.C., 2012. *Soil Microbial Biomass in the Amazon, Atlantic Forest and Antarctica*. PhD Thesis, Universidade Federal Rural do Rio de Janeiro (97 f).

Maag, M., Vinther, F.P., 1999. Effect of temperature and water on gaseous emissions from soils treated with animal slurry. *Soil Sci. Soc. Am. J.* 63, 858–865.

Madigan, M.T., Martinko, J.M., Dunlap, P.V., Clark, D.P., 2010. *Brock Biology of Microorganisms*. 12th ed. Artmed, Porto Alegre.

Magrin, G.O., Marengo, J.A., Boulanger, J.-P., Buckeridge, M.S., Castellanos, E., Poveda, G., Scarano, F.R., Vicuña, S., 2014. Central and South America. In: Barros, V.R., Field, C.B., Dokken, D.J., Mastrandrea, M.D., Mach, K.J., Bilir, T.E., Chatterjee, M., Ebi, K.L., Estrada, Y.O., Genova, R.C., Girma, B., Kissel, E.S., Levy, A.N., MacCracken, S., Mastrandrea, P.R., White, L.L. (Eds.), *Climate Change 2014: Impacts, Adaptation, and Vulnerability. Part B: Regional Aspects*. Contribution of Working Group II to the Fifth Assessment Report of the Intergovernmental Panel on Climate Change. Cambridge University Press, Cambridge, United Kingdom and New York, NY, USA, pp. 1499–1566.

Michaelson, G.J., Dai, X.Y., Ping, C.L., 2004. Organic matter and bioactivity in cryosols of Arctic Alaska. In: Kimble, J.M. (Ed.), *Cryosols, Permafrost-affected Soils*, pp. 463–479.

Michel, R.F.M., Schaefer, C.E.G.R., Dias, L., Simas, F.N.B., Benites, V., Mendonça, E.S., 2006. Ornithogenic gelisols (Cryosols) from maritime Antarctica: pedogenesis, vegetation and carbon studies. *Soil Sci. Soc. Am. J.* 70, 1370–1376.

Miyazawa, M., Pavan, M.A., Block, M.F., 1985. Spectrophotometry determination of nitrate in soil extracts without chemical reduction (in Portuguese). *Pesq. Agrop. Brasileira* 20, 129–133.

Mosier, A., Wassmann, R., Verchot, L., King, J., Palm, C., 2004. Methane and nitrogen oxide flux in tropical agricultural soils: sources, sinks and mechanisms. *Environ. Dev. Sustain.* 6, 11–49.

Oechel, W.C., Billings, W.D., 1992. Effects of global change on the Carbon balance of Arctic plants and ecosystems. In: Chapin, F.I.I.F.S., Jefferies, R.L., Reynolds, J.F., Shaver, G.R., Svoboda, J. (Eds.), *Arctic Ecosystems in a Changing Climate*. Academic Press, Inc, pp. 139–168.

Olajuuyigbe, S., Tobin, B., Saunders, M., Nieuwenhuis, M., 2012. Forest thinning and soil respiration in a Sitka spruce forest in Ireland. *Agric. For. Meteorol.* 157, 86–95. <https://doi.org/10.1016/j.agrformet.2012.01.016>.

O'Neill, A.L., Kupiec, J.A., Curran, P.J., 2002. Biochemical and reflectance variation throughout a Sitka spruce canopy. *Remote Sens. Environ.* 80, 134–142.

Orchard, V.A., Corderoy, D.M., 1983. Influence of environmental factors on the decomposition of penguin guano in Antarctica. *Polar Biol.* 1, 199–204.

Pérez, T., Trumbore, S.E., Tyler, S.C., Davidson, E.A., Keller, M., de Camargo, P.B., 2000. Isotopic variability of N₂O emissions from tropical forest soils. *Glob. Biogeochem. Cycles* 14, 525–535.

Peri, P.L., Lencinas, M.V., Pastur, G.J.M., Lasagno, R., 2013. Diversity patterns in the steppe of Argentinean southern Patagonia: environmental drivers and impact of grazing. In: Morales Prieto, M.B., TrabaDíaz, J. (Eds.), *Steppe Ecosystems: Biological Diversity, Management and Restoration*. 4. NOVA Science Publishers Inc, New York, US, pp. 73–95.

Pires, C.V., Schaefer, C., Hashigushi, A.K., Thomazini, A., Filho, E.I.F., Mendonça, E.S., 2017. Soil organic carbon and nitrogen pools drive soil C–CO₂ emissions from selected soils in maritime Antarctica. *Sci. Total Environ.* 596, 124–135.

Post, W.M., Emanuel, W.R., Zinke, P.J., Stangenberger, A.G., 1982. Soil carbon pools and world life zones. *Nature* 298 (5870), 156–159.

Poth, M., Focht, D.D., 1985. 15N kinetic analysis of N₂O production by Nitrosomonas europaea: an examination of nitrifier denitrification. *Appl. Environ. Microbiol.* 49, 1134–1141.

Price, Sally J., Kelliher, Francis M., Sherlock, Robert R., Tate, Kevin R., Condron, Leo M., 2004. Environmental and chemical factors regulating methane oxidation in a New Zealand forest soil. *Aust. J. Soil Res.* 42, 767–776.

Puigdefàbregas, J., Del Barrio, G., Iturraspe, R., 1988. Régimen térmico estacional de un ambiente montañoso en la Tierra del Fuego, con especial atención al límite superior del bosque. *Pirineos* 132, 37–48.

Rodella, A.A., Alcarde, J.C., 1994. Avaliação de materiais orgânicos empregados como fertilizantes. *Sci. Agric.* 51, 556–562.

Rowlings, D.W., Grace, P.R., Scheer, C., Kiese, R., 2013. Influence of nitrogen fertiliser application and timing on greenhouse gas emissions from a lychee (*Litchi chinensis*) orchard in humid subtropical Australia. *Agric. Ecosyst. Environ.* 179, 168–178. <https://doi.org/10.1016/j.agee.2013.08.013>.

Saggars, S., Hedley, C.B., Giltrap, D.L., Lambie, S.M., 2007. Measured and modeled estimates of nitrous oxide emission and methane consumption from a sheep-grazed pasture. *Agric. Ecosyst. Environ.* 122, 357–365.

Schaufler, G., Kitzler, B., Schindlbacher, A., Skiba, U., Sutton, M.A., Zechmeister-Boltenstern, S., 2010. Greenhouse gas emissions from European soils under different land use: effects of soil moisture and temperature. *Eur. J. Soil Sci.* 61, 683–696.

Simas, F.N.B., Schaefer, C.E.G.R., Melo, V.F., Albuquerque Filho, M.R., Michel, R.F.M., Pereira, V.V., Gomes, M.R.M., Costa, L.M., 2007. Ornithogenic Cryosols from Maritime Antarctica: Phosphatization as Soil Forming Process. 138. *Geoderma*, Amsterdam, pp. 191–203.

Simas, F.N.B., Schaefer, C.E.G.R., Filho, Albuquerque, de, M.R., Francelino, M.R.A., Filho, Fernandes, Gilkes, R.J., da Costa, L.M., 2008. Genesis, Properties and Classification of Cryosols from Admiralty Bay, Maritime Antarctica. 144. *Geoderma*, Amsterdam, pp. 116–122.

Smith, K.A., et al., 2003. Exchange of greenhouse gases between soil and atmosphere: interactions of soil physical factors and biological processes. *Eur. J. Soil Sci.* 54, 779–791.

Smith, P., Martino, D., Cai, Z., Gwary, D., Janzen, H., Kumar, P., McCarl, B., Ogle, S., O'Mara, F., Rice, C., Scholes, B., Sirotenko, O., Howden, M., McAllister, T., Pan, G., Romanenkov, V., Schneider, U., Towprayoon, S., Wattenbach, M., Smith, J., 2008. Greenhouse gas mitigation in agriculture. *Phil. Trans. R. Soc. B* 363, 789–813. <https://doi.org/10.1098/rstb.2007.2184>.

Soil Survey Staff, 2014. *Keys to Soil Taxonomy*. 12th ed. USDA-NRCS, Washington, DC (370 p.).

Steudler, P.A., Melillo, J.M., Feigl, B.J., Neill, C., Piccolo, M.C., Cerri, C.C., 1996. Consequence of forest-to-pasture conversion on CH₄ fluxes in the Brazilian Amazon. *J. Geophys. Res.* 101 (D13), 18547–18554.

Stoffel, M., Bollschweiler, M., Butler, D.R., Luckman, B.H., 2010. *Tree Rings and Natural Hazards: a State-of-art*. Heidelberg Springerpg (505p).

Strelin and Iturraspe, 2007. Recent evolution and mass balance of Cordón martial glaciers, cordillera Fueguina oriental. *Glob. Planet. Chang.* 59, 17–26.

Sun, L.G., Zhu, R.B., Xie, Z.Q., Xing, G.X., 2002. Emissions of nitrous oxide and methane from Antarctic tundra: role of penguin droppings deposition. *Atmos. Environ.* 36, 4977–4982.

Takakai, F., Desyatkin, A.R., Lopez, C.M.L., Fedorov, A.N., Desyatkin, R.V., Hatano, R., 2008. CH₄ and N₂O emissions from a forest-alas ecosystem in the permafrost taiga forest region, eastern Siberia, Russia. *J. Geophys. Res.* 113, G02002. <https://doi.org/10.1029/2007JG000521>.

Thomazini, A., Mendonça, S., Teixeira, D.B., Almeida, I.C.C., La Scala, N., Canellas, L.P., Spokas, K.A., Milori, D., Turbay, C.V.G., Fernandes, R.B.A., Schaefer, C., 2015. CO₂ and N₂O emissions in a soil chronosequence at a glacier retreat zone in maritime Antarctica. *Sci. Total Environ.* 521, 336–345.

Thomazini, A., Francelino, M.R., Pereira, A.B., Schuenemann, A.L., Mendonça, E.S., Almeida, P.H.A., Schaefer, C., 2016. Geospatial variability of soil CO₂-C exchange in the main terrestrial ecosystems of Keller Peninsula, Maritime Antarctica. *Sci. Total Environ.* 562, 802–811.

Tuhkanen, S., 1992. The climate of Tierra del Fuego from a vegetation geographical point of view and its ecoclimatic counterparts elsewhere. *Acta Bot. Fenn.* 145, 1–64.

Ullah, S., 2009. Co-integration and causality between exports and economic growth in Pakistan. *Eur. J. Soil Sci.* 10 (2), 264–272.